

Efficient conversion of fructose to 5-hydroxymethylfurfural by functionalized γ -Al₂O₃ beads

Fang Lin¹  | Kang Wang¹  | Lan Gao² | Xin Guo²
¹Tianjin Key Lab of Membrane Science and Desalination Technology, Chemical Engineering Research Center, School of Chemical Engineering and Technology, Tianjin University, Tianjin 300350, China

²Research Institute of Petroleum Processing, SINOPEC, Beijing 100013, China

Correspondence

Kang Wang, Tianjin Key Lab of Membrane Science and Desalination Technology, Chemical Engineering Research Center, School of Chemical Engineering and Technology, Tianjin University, Tianjin, 300350, China.
Email: 18322693646@163.com

Funding information

Natural Science Foundation of Tianjin, China, Grant/Award Number: 16JCYBJC19600; National Key R&D Program of China, Grant/Award Number: 2017YFB0306502

Millimeter size γ -Al₂O₃ beads were prepared by alginate assisted sol-gel method and grafting organic groups with propyl sulfonic acid and alkyl groups as functionalized γ -Al₂O₃ bead catalysts for fructose dehydration to 5-hydroxymethylfurfural (5-HMF). Experiment results showed that the porous structure of γ -Al₂O₃ beads was favorable to the loading and dispersion of active components, and had an obvious effect on the properties of the catalyst. The lower calcination temperature of γ -Al₂O₃ beads increased the specific surface area, the hydrophobicity and the activity of catalysts. Competition between the reaction of alkyl groups and -SH groups with surface hydroxyl during the preparation process of the catalyst influenced greatly the acid site densities, hydrophobic properties and activity of the catalyst. With an increase in the alkyl group chain, the hydrophobicity of catalysts increased obviously and the activity of the catalyst was enhanced. The most hydrophobic catalyst C₁₆-SO₃H- γ -Al₂O₃-650°C exhibited the highest yield of 5-HMF (84%) under the following reaction conditions: reaction medium of dimethylsulfoxide/H₂O (V/V, 4:1), catalyst amount of 30 mg, temperature of 110°C and reaction time of 4 hr.

KEYWORDS

5-hydroxymethylfurfural, calcination temperature, fructose, functionalized γ -Al₂O₃ bead, pore structure

1 | INTRODUCTION

Among various biomass-derived valuable chemicals reported to date, because 5-hydroxymethylfurfural (5-HMF) is easily converted into a variety of high-value-added chemicals, it is regarded as a key platform compound, such as, 2,5-diformylfuran (2,5-DFP),^[1,2] 2,5-furandicarboxylic acid (2,5-FDCA),^[3,4] C₉-C₁₅ alkanes^[5] and others.^[6] In addition, levulinic acid, the hydrolysate of HMF, can be converted into methyl tetrahydrofuran (MTHF) as a gasoline additive.^[7] Therefore, the study of the transformation of biomass into 5-HMF has received considerable attention. However, there were obstacles in the preparation process of 5-HMF, including the selection of catalysts and solvents, which affect its yield and

selectivity, and directly decide the prospect of industrial production.

As reported previously, fructose has been studied widely as a starting material for the production of HMF due to its high activity and efficiency towards HMF production. In recent years, the dehydration of fructose into 5-HMF has shown a rapid progression in developing catalytic systems. In this process, many people study homogeneous catalytic systems, such as mineral acids,^[8] metal halides^[9] or organic acids,^[10] which have shown moderate yields (40–60%) of 5-HMF. At the same time, there are several serious drawbacks, such as separation of the products, recycling of catalysts, and the corrosion of materials, which are not conducive to large-scale industrial production. Recently, it was reported that EDTA

was an efficient organic acid catalyst that could improve HMF yield up to $89 \pm 3\%$, and could be easily recycled by cooling the reaction mixture to room temperature. However, further experiments are necessary to investigate its potential in practical applications.^[11] In contrast, heterogeneous acid catalysts that avoid the aforementioned disadvantage have been widely utilized for biomass conversion into 5-HMF, such as supported heteropoly acids,^[12,13] metal phosphates,^[14] cation exchange resins,^[15,16] sulfated zirconia,^[17] Metal Organic Framework (MOFs),^[18] acid-functionalized silicas,^[19,20] and C-based solid acids.^[21–23] They have the advantage of being easily separated and recyclable, making them more suitable for industrial production applications.

Furthermore, both the yield of 5-HMF and selectivity depend greatly on the reaction medium. Wang *et al.* suggested that the strong interaction between solvents and beta zeolite (H β) has a crucial influence on the catalytic performance, and also suggested an effective approach to improving the selectivity by regulating the solvents.^[24] It was shown that high yields and selectivity of 5-HMF can be obtained in ionic liquids^[25] and some organic solvents, such as dimethylsulfoxide (DMSO).^[26,27] Indeed, the use of ionic liquids can not only improve the selectivity of HMF because of its extraction with 5-HMF, but also reaction rates were increased, and levulinic acid and humin side-products were not formed.^[28] Nonetheless, from the view of industrial application cost, most ionic liquids are expensive and unsuitable for mass production. DMSO has an important positive effect on the reaction mainly because of the following aspects. First, it facilitates the formation of the furanoid form of fructose, which can be easily dehydrated to HMF. Second, DMSO can act as both an electron acceptor and an electron donor to improve the dehydration of the sugars. Third, DMSO can prevent the formation of byproducts such as levulinic acid and humins from HMF. Moreover, as a versatile polar aprotic solvent, DMSO can dissolve both polar and non-polar compounds, which makes it an effective solvent for sugars and the products.

However, aqueous systems are more economically and environmentally friendly as solvents for 5-HMF production. Unfortunately, water as a reaction medium was conducive to side-effects, such as the conversion of HMF unstable intermediates into polymers, humins and 5-HMF rapid rehydration into levulinic acid, formic acid, etc., resulting in low 5-HMF selectivity and yield in aqueous media.^[19] So, in order to improve the 5-HMF yield and further reduce the cost of application, biphasic solvent systems appeared. For instance, Román-Leshkov *et al.* studied the effect of a two-phase reaction solvent containing primary alcohols, diketones and others on the dehydration of fructose to HMF. They demonstrated

that thiol groups promote the isomerization of fructose to form furanose, and favor the dehydration reaction.^[29,30] In the two-phase catalytic system, the product 5-HMF was continuously extracted from the aqueous phase into the organic phase. So the rehydration of 5-HMF can hardly proceed because of its separation from water in a large extent. Lv *et al.* introduced MIBK into the reaction system, which can extract HMF into the MIBK phase, improve HMF selectivity in the reaction, and suppress the formation and deposition of humins on the catalyst surface.^[31] It can be seen from the process of solvent use, that blocking the rehydration of 5-HMF was an important means to enhance the yield and selectivity, therefore the use of hydrophobic solid catalyst has been studied. Wang *et al.* synthesized a superhydrophobic acid catalyst (P-SO₃H-154) for fructose dehydration to 5-HMF, and the yield of 5-HMF as the sole product increased to 99% in the three-phase solvent system.^[32] They believed that stabilizing 5-HMF and inhibiting rehydration of 5-HMF was due to the isolation of the acid sites in the catalyst from the oxygen atom of water molecules in the reaction system. Recently, Yang *et al.* ingeniously designed a series of hydrophobic silica nanoparticle catalysts, which also successfully restrained the rehydration of 5-HMF in the DMSO–water solvent system, thereby improving the 5-HMF yield and selectivity.^[33]

These catalyst systems can largely improve the 5-HMF yield and selectivity, but there are still some problems such as the recovery, and utilization operation of powder catalysts is relatively complex. Yao *et al.* designed a magnetically recoverable carbonaceous material catalyst, which could be recovered by an external magnetic field after reaction.^[34] Nevertheless, there was also a certain catalyst loss and high cost of industrial production in the recovery process. It was important to develop a more efficient catalytic system for the industrial production of 5-HMF with lower cost and better performance.

In recent years, aluminum oxide (Al₂O₃) was an abundant, cheap and commercially available material. Due to its various forms, good thermal stability, high specific surface and acid surface, and easy to be functionalized by various functional groups, it has been widely used in the field of catalysis. For example, some researchers control the acidity of the alumina by using inorganic acid groups.^[35,36] Furthermore, the alumina has abundant superficial hydroxyl groups, which were adequate for some functionalization of functional groups and modifying the acidity.^[37] Recently, De la Rosa and co-workers synthesized an organic group-modified alumina by the sol–gel method, and grafted thiol and sulfonic groups.^[38,39] After 24 hr of continuous reaction, the loss of sulfur content in the catalyst was 15%, and the fructose conversion yield and selectivity to 5-HMF

did not undergo significant changes (less than 5%), which showed an efficient stability of the catalyst.^[39]

Herein, in order to overcome the problem of the recovery of powder catalyst and improve the performance of the catalyst, millimeter size γ -Al₂O₃ beads (1.8 mm) prepared by the alginate assisted sol-gel method^[40,41] were used as supports and modified with propyl sulfonic acid and alkyl groups as functionalized γ -Al₂O₃ bead catalyst. The effects of the preparation process, such as alkylation, sulfonation and calcination temperature of γ -Al₂O₃ beads on the pore structure, acidity, hydrophobicity and activity of catalyst were investigated by scanning electron microscopy (SEM), Brunauer-Emmett-Teller (BET), Fourier transform-infrared (FT-IR) analysis, energy-dispersive X-ray spectroscopy (EDS), acid-base titration[S1], water contact angles (CAs) and the dehydration of fructose into 5-HMF. The optimization of reaction conditions and the reusability of the catalyst were also presented.

2 | RESULTS AND DISCUSSION

2.1 | Characterization of the functionalized γ -Al₂O₃ beads

2.1.1 | Morphology of catalysts

As shown in Figure 1, the C₁₆-SO₃H- γ -Al₂O₃-650°C were white, smooth surface, uniform in size with about 1.8 mm, and can be directly used as fillers in industrial production, which was in accordance with the appearance of γ -Al₂O₃ beads. Table 1 showed that the crush strength of the catalyst decreased after alkylation and sulfonation. However, the crush strength of all catalysts was over 36 N per bead, which could satisfy the requirement of practical application.

In order to understand the surface and cross-section morphology of functionalized γ -Al₂O₃ beads, the samples



FIGURE 1 Optical photo of C₁₆-SO₃H- γ -Al₂O₃-650°C

were analyzed by SEM. As indicated in Figure 2, the surface and cross-section morphology of γ -Al₂O₃-650°C beads were loose porous structure, and rich macropore in micron size and mesoporous structure could be observed. The macroporous number of SO₃H- γ -Al₂O₃-650°C beads was significantly reduced. After being loaded with alkylation reagents, the skeleton structure of functionalized γ -Al₂O₃ beads became pyknotic. It was demonstrated that both the surface and the interior of the beads have been alkylated and sulfonated successfully. When the calcination temperature of the support increased to 1000°C, the section morphology of C₁₆-SO₃H- γ -Al₂O₃-1000°C became flatter, which inferred a reduction in specific surface area.

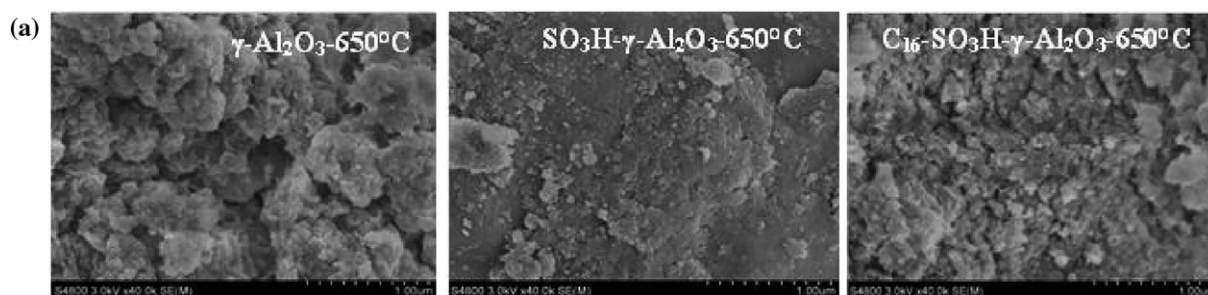
2.1.2 | Pore distribution of catalysts

The pore structure of the catalyst, especially the specific surface area, is closely related to its activity and selectivity. Figure 3 showed the effects of modification on the distribution of the pore size of γ -Al₂O₃ beads. It can be seen from Figure 3 that the pore distribution peak shifts to small pore after the sulfonation of Al₂O₃-650°C beads, which indicates that the acidification process caused a certain damage to the macropore structure of the alumina particles and promoted the formation of small pores. However, when alkylation was carried out prior to the sulfonation process, the pore distribution peak of C₃-SO₃H- γ -Al₂O₃ moved to large pores, and that of C₈-SO₃H- γ -Al₂O₃ was close to that of γ -Al₂O₃ beads. Furthermore, the pore distribution area of C₁₆-SO₃H- γ -Al₂O₃ was reduced obviously because of the blockage of pores by long alkanes. It seems that the alkylation reaction depresses the destruction of aluminum pore structure by sulfonation reaction. The catalyst with larger average pore size was beneficial to the diffusion of the reactants.

Table 1 showed the BET data of samples. It can be seen clearly that the specific surface area of SO₃H- γ -Al₂O₃-650°C increased and that of C₁₆-SO₃H- γ -Al₂O₃-650°C decreased due to the blockage of pores by long alkanes. When the catalyst was only sulfonated, both the pore volume and the average pore diameter were reduced, which indicated that the pore structure of the catalyst was destroyed. However, the longer alkyl chain grafted to the γ -Al₂O₃ beads, the greater steric hindrance for grafting of organic -SO₃H groups, the pore volume and average pore diameter of the catalyst gradually increased. This was consistent with the results from Figure 3 that the alkylation reaction protected from the damage of aluminum pore structure under strong acidity treatment.

TABLE 1 The crush strength and BET data of samples

Sample	Crush strength (N per bead)	Specific surface area ($\text{m}^2 \text{g}^{-1}$)	Pore volume ($\text{cm}^3 \text{g}^{-1}$)	Average pore diameter (nm)
$\gamma\text{-Al}_2\text{O}_3\text{-650}^\circ\text{C}$	56.8	211.5	0.5259	9.947
$\text{SO}_3\text{H-}\gamma\text{-Al}_2\text{O}_3\text{-650}^\circ\text{C}$	39.4	280.6	0.4503	6.419
$\text{C}_3\text{-SO}_3\text{H-}\gamma\text{-Al}_2\text{O}_3\text{-650}^\circ\text{C}$	37.0	259.0	0.4679	7.226
$\text{C}_8\text{-SO}_3\text{H-}\gamma\text{-Al}_2\text{O}_3\text{-650}^\circ\text{C}$	36.5	259.1	0.5088	7.856
$\text{C}_{16}\text{-SO}_3\text{H-}\gamma\text{-Al}_2\text{O}_3\text{-650}^\circ\text{C}$	38.4	176.3	0.5418	8.435
$\text{C}_{16}\text{-SO}_3\text{H-}\gamma\text{-Al}_2\text{O}_3\text{-650}^\circ\text{C}$ (the fifth cycle)	36.9	170.2	0.5048	8.246
$\gamma\text{-Al}_2\text{O}_3\text{-850}^\circ\text{C}$	68.6	182.8	0.4858	10.630
$\text{C}_{16}\text{-SO}_3\text{H-}\gamma\text{-Al}_2\text{O}_3\text{-850}^\circ\text{C}$	65.5	167.7	0.4583	10.221
$\gamma\text{-Al}_2\text{O}_3\text{-1000}^\circ\text{C}$	65.3	137.9	0.4743	16.090
$\text{C}_{16}\text{-SO}_3\text{H-}\gamma\text{-Al}_2\text{O}_3\text{-1000}^\circ\text{C}$	46.5	121.5	0.4143	13.642

**FIGURE 2** (a) Scanning electron microscopy (SEM) images of the surface of different functionalized $\gamma\text{-Al}_2\text{O}_3$ beads. (b) SEM images of the cross-section of different functionalized $\gamma\text{-Al}_2\text{O}_3$ beads

In addition, the calcination temperature obviously affects the pore structure of supports. The small hole of alumina supports collapse into the large hole under high-temperature calcinations, which lessens the specific surface area of alumina supports and catalysts in Table 1.

2.1.3 | Surface functional groups of catalysts

In order to investigate the surface functional groups of the as-prepared catalysts, FT-IR analysis was carried out. As shown in Figure 4, for $\gamma\text{-Al}_2\text{O}_3\text{-650}^\circ\text{C}$ beads, the absorption bands at 3456 cm^{-1} (O-H stretching vibration), 1650 cm^{-1} (O-H bending vibration),^[38] 1536 cm^{-1} and 1434 cm^{-1} (Al-O group) were observed. After the addition of functional groups, IR bands at about 2928 cm^{-1} and 2846 cm^{-1} ascribed to the stretching vibration of CH_2 in the hydrocarbon chain,^[42] and 1170 cm^{-1} and 1098 cm^{-1} attributed to the characteristic adsorption of $-\text{SO}_3\text{H}$ groups^[43] were detected, indicating that surface functional

groups were incorporated successfully, and $-\text{SH}$ groups were converted to $-\text{SO}_3\text{H}$ groups. As the grafted alkyl chain length increases, the $-\text{CH}_2$ vibrational bands at approximately 2928 and 2846 cm^{-1} became strong, and $-\text{SO}_3\text{H}$ groups vibrational bands at 1170 cm^{-1} and 1098 cm^{-1} decreased. Yang considered that the phenomenon was caused by steric hindrance in the structure, the longer alkyl chain grafted to the $\gamma\text{-Al}_2\text{O}_3$ beads, the greater steric hindrance for grafting of organic $-\text{SO}_3\text{H}$ groups.^[33] This experimental result was also in agreement with that of pore distribution, i.e. the alkylation reaction depresses the destruction of aluminum pore structure by sulfonation reaction.

Moreover, the calcination temperature also influenced the load of functional groups. With the increase of calcination temperature, the stretching vibration of CH_2 became weaker and that of $-\text{SO}_3\text{H}$ enhanced. It was well known that the specific surface area and the active hydroxyl groups of alumina were reduced with an increase in calcination temperature, which led to a decrease in the number of cross-linked trimethoxy and

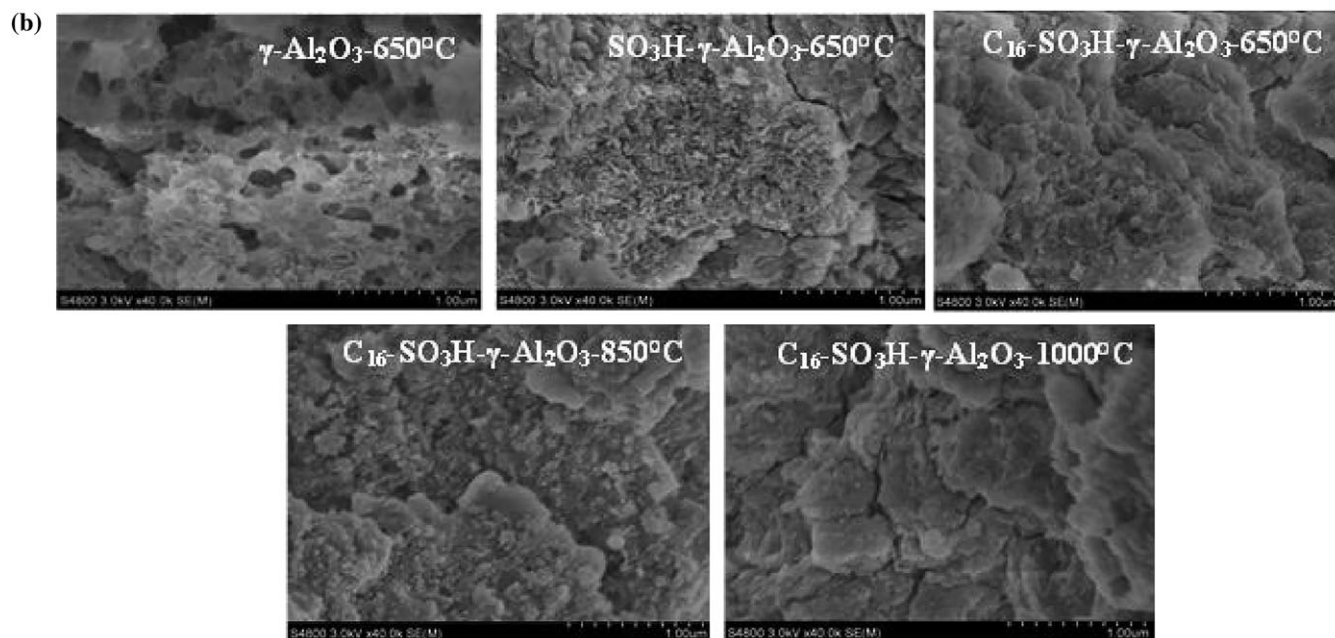


FIGURE 2 Continued.

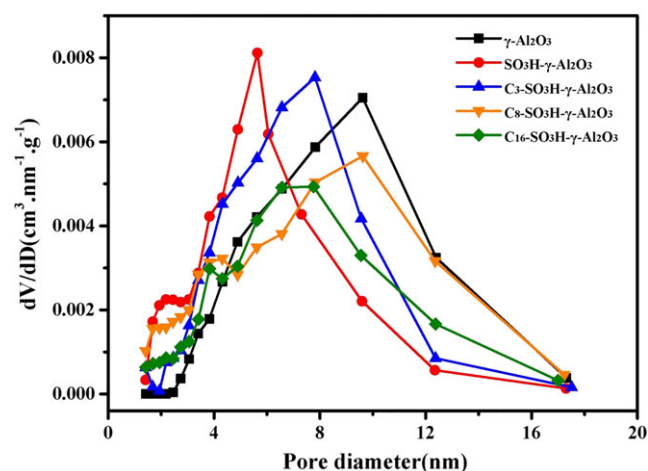


FIGURE 3 Distribution of pore size

CH₂, then relatively more -SO₃H were loaded in the subsequent sulfonation process.

To verify the above results, the element analysis results of catalysts by EDS were shown in Table 2. With the increase in carbon chain length of the alkylation reagent, the content of C increased, but that of S decreased. After alkylation, steric hindrance of long-chain alkanes led to lessen the subsequent -SH binding with supports. In addition, under higher calcination temperature, C content decreased and S content increased, at the same time the total content of C and S reduced, which was mainly due to the competition between alkyl chain and -SH groups and the reduction of hydroxyl groups on alumina. These results were in accordance with those of FT-IR analysis.

Moreover, as listed in Table 2, S and C were detected on the outer and inner surface of the catalyst, showing that the functional groups were loaded successfully on the outer surface and inside of the pore, which was consistent with the experimental results by SEM.

The acid site densities and hydrophobic properties of catalysts were related to S and C content of catalysts, respectively. The acid site densities were determined by acid-base titration using NaOH[S1], as listed in Table 2. Obviously, the acid site densities agreed well with the S content of catalysts, and the values of acid site density/S content on the catalyst cross-section were in the range of 29.4–30.5 mmol g⁻¹ (g indicates the quality of the S element), which remains approximately constant, indicating that the acid sites mainly resulted from SO₃H groups. With the increase in alkyl chain length, the acid site density gradually decreased due to the reduction of S content. In addition, the increase of calcination temperature for γ-Al₂O₃ beads can raise S content and enhance acid site density. This result is ascribed to the decrease of C content. In order to ensure the consistency of the ratio of acid density and substrate, the mass ratio of functionalized γ-Al₂O₃ beads used in the following fructose dehydration reactions was adjusted according to their acidity densities.

To study the hydrophobic properties of functionalized γ-Al₂O₃ beads, samples were dispersed in the two-phase solvent system containing dichloromethane and water, respectively. As shown in Figure 5, SO₃H-γ-Al₂O₃-650°C and C₃-SO₃H-γ-Al₂O₃-650°C beads stayed in the oil-water interface and were unable to enter the oil phase, while C₈-SO₃H-γ-Al₂O₃-650°C and C₁₆-SO₃H-γ-Al₂O₃-

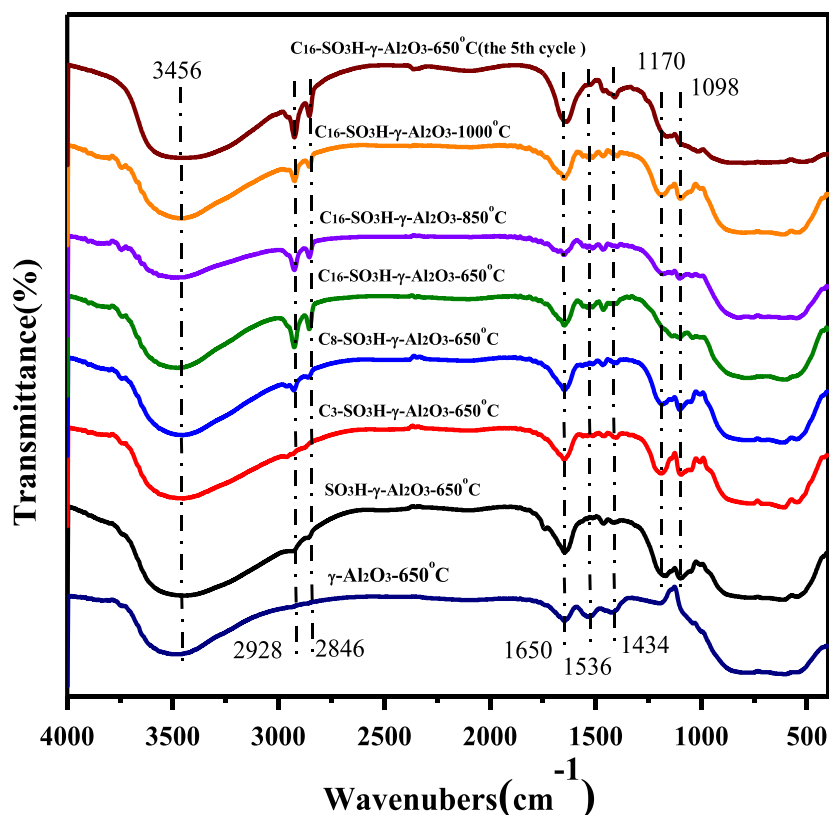









FIGURE 4 Fourier transform-infrared (FT-IR) spectra of functionalized γ - Al_2O_3 beads

TABLE 2 The S and C content, and the surface properties of catalysts

Sample	S content (wt%) Surface/cross-section	C content (wt%) Surface/cross-section	Acid site density (mmol g^{-1})	CA	Photo of water CA
$\text{SO}_3\text{H}-\gamma\text{-Al}_2\text{O}_3\text{-}650^\circ\text{C}$	2.25/1.82	28.2/25.2	0.55	17.1°	
$\text{C}_3\text{-SO}_3\text{H}-\gamma\text{-Al}_2\text{O}_3\text{-}650^\circ\text{C}$	1.38/1.16	35.0/32.0	0.35	32.8°	
$\text{C}_8\text{-SO}_3\text{H}-\gamma\text{-Al}_2\text{O}_3\text{-}650^\circ\text{C}$	1.26/1.05	44.0/43.6	0.32	54.9°	
$\text{C}_{16}\text{-SO}_3\text{H}-\gamma\text{-Al}_2\text{O}_3\text{-}650^\circ\text{C}$	1.13/1.02	61.6/60.0	0.30	88.4°	
$\text{C}_{16}\text{-SO}_3\text{H}-\gamma\text{-Al}_2\text{O}_3\text{-}650^\circ\text{C}$ (the fifth cycle)	1.09/0.98	61.0/59.6	0.29	83.5°	
$\text{C}_{16}\text{-SO}_3\text{H}-\gamma\text{-Al}_2\text{O}_3\text{-}850^\circ\text{C}$	1.30/1.07	52.9/47.8	0.32	45.3°	
$\text{C}_{16}\text{-SO}_3\text{H}-\gamma\text{-Al}_2\text{O}_3\text{-}1000^\circ\text{C}$	1.72/1.34	48.8/47.9	0.41	38.6°	

CA, contact angle.

650°C beads completely sank in the bottom of dichloromethane. This phenomenon showed intuitively that the increase in alkyl chain length greatly enhanced the hydrophobicity of the catalyst. In order to further quantitatively compare the hydrophobicity of functionalized γ - Al_2O_3 beads, the water droplet CAs were measured. As shown in Table 2, the water CA for $\text{SO}_3\text{H}-\gamma\text{-Al}_2\text{O}_3\text{-}$

650°C in pure water was about 17.1° , and this increased gradually to 32.8° , 54.9° and 88.4° with the increase in alkyl chain from C_3 to C_{16} , respectively. This could be attributed to different hydrophobic properties of the alkyl chain. Because the hydrophobic properties of the catalyst helped in stabilizing 5-HMF and inhibiting rehydration of 5-HMF due to the isolation of the acid sites in the catalyst

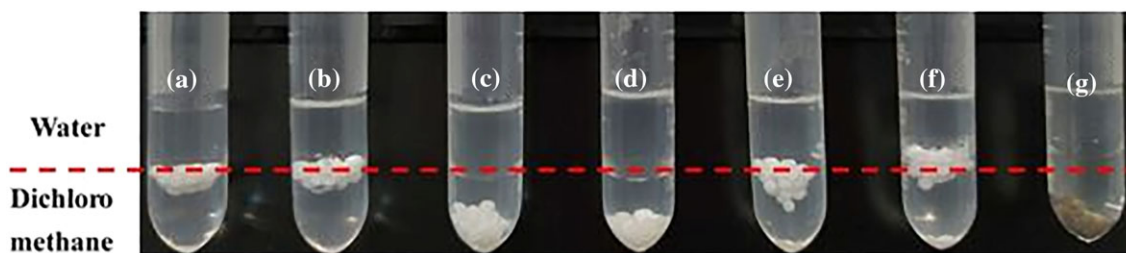


FIGURE 5 Macro picture for dispersion of (a) $\text{SO}_3\text{H}-\gamma\text{-Al}_2\text{O}_3-650^\circ\text{C}$, (b) $\text{C}_3\text{-SO}_3\text{H}-\gamma\text{-Al}_2\text{O}_3-650^\circ\text{C}$, (c) $\text{C}_8\text{-SO}_3\text{H}-\gamma\text{-Al}_2\text{O}_3-650^\circ\text{C}$, (d) $\text{C}_{16}\text{-SO}_3\text{H}-\gamma\text{-Al}_2\text{O}_3-650^\circ\text{C}$, (e) $\text{C}_{16}\text{-SO}_3\text{H}-\gamma\text{-Al}_2\text{O}_3-850^\circ\text{C}$, (f) $\text{C}_{16}\text{-SO}_3\text{H}-\gamma\text{-Al}_2\text{O}_3-1000^\circ\text{C}$ and (g) $\text{C}_{16}\text{-SO}_3\text{H}-\gamma\text{-Al}_2\text{O}_3-650^\circ\text{C}$ (the fifth cycle) in the two-phase system of water and dichloromethane

from the oxygen atom of water molecules in the reaction system, the alkylation of the catalyst would bring benefit to dehydration of fructose into 5-HMF.

In addition, the hydrophobicity of the catalyst decreased by using high-temperature calcined $\gamma\text{-Al}_2\text{O}_3$ beads as supports. As shown in Figure 5, the higher the calcination temperature, the less $\gamma\text{-Al}_2\text{O}_3$ beads are dispersed in the oil phase. It was also found from Table 2 that the water CAs of the catalyst with high-temperature calcinations decreased. The main reason was the reduction of grafting alkyl chain content when $\gamma\text{-Al}_2\text{O}_3$ beads were calcined at high temperature.

The relationship between surface functional group and pore structure was further discussed. It can be seen from BET data in Table 1 that the specific surface area of the catalyst decreases with an increase in the length of the carbon chain, which should not benefit improving the hydrophobicity of the catalyst, but the hydrophobicity of catalyst increased. Thus, the contribution of carbon chain increase was a critical factor. Of course, the surface area and pore volume of supports should not be too small to ensure that the catalyst has enough catalytic surface. Furthermore, for the catalysts with the same carbon chain, $\text{C}_{16}\text{-SO}_3\text{H}-\gamma\text{-Al}_2\text{O}_3$ system, the decrease of specific surface area of catalysts by using a high calcination temperature will reduce the hydrophobicity of the catalyst.

2.2 | Catalytic performances

2.2.1 | Effect of alkyl chain length on dehydration of fructose into 5-HMF

The four functionalized $\gamma\text{-Al}_2\text{O}_3$ beads ($\text{SO}_3\text{H}-\gamma\text{-Al}_2\text{O}_3-650^\circ\text{C}$, $\text{C}_3\text{-SO}_3\text{H}-\gamma\text{-Al}_2\text{O}_3-650^\circ\text{C}$, $\text{C}_8\text{-SO}_3\text{H}-\gamma\text{-Al}_2\text{O}_3-650^\circ\text{C}$ and $\text{C}_{16}\text{-SO}_3\text{H}-\gamma\text{-Al}_2\text{O}_3-650^\circ\text{C}$) as solid acids were used to evaluate the fructose dehydration to 5-HMF. In order to ensure the consistency of acid density and fructose ratio in these parallel experiments, the catalyst amount was 20, 25, 30 and 30 mg, respectively, for $\text{SO}_3\text{H}-\gamma\text{-Al}_2\text{O}_3-650^\circ\text{C}$, $\text{C}_3\text{-SO}_3\text{H}-\gamma\text{-Al}_2\text{O}_3-650^\circ\text{C}$, $\text{C}_8\text{-SO}_3\text{H}-\gamma\text{-Al}_2\text{O}_3-650^\circ\text{C}$ and $\text{C}_{16}\text{-SO}_3\text{H}-\gamma\text{-Al}_2\text{O}_3-650^\circ\text{C}$. In addition, the $\gamma\text{-Al}_2\text{O}_3$ beads were also used as blank experiments. The effect of the hydrophobicity of functionalized $\gamma\text{-Al}_2\text{O}_3$ beads on the dehydration of fructose to 5-HMF was shown in Figure 6. The $\gamma\text{-Al}_2\text{O}_3$ beads as catalyst had a low 5-HMF yield. But the yields of 5-HMF obtained with $\text{SO}_3\text{H}-\gamma\text{-Al}_2\text{O}_3-650^\circ\text{C}$, $\text{C}_3\text{-SO}_3\text{H}-\gamma\text{-Al}_2\text{O}_3-650^\circ\text{C}$, $\text{C}_8\text{-SO}_3\text{H}-\gamma\text{-Al}_2\text{O}_3-650^\circ\text{C}$ and $\text{C}_{16}\text{-SO}_3\text{H}-\gamma\text{-Al}_2\text{O}_3-650^\circ\text{C}$ were 52%, 66%, 70% and 84%, respectively, which indicates that the hydrophobic properties of the functionalized $\gamma\text{-Al}_2\text{O}_3$ beads could increase the yield of 5-HMF, the stronger the hydrophobicity the higher the yield of 5-HMF. This reaction further confirmed that hydrophobic groups in the $\gamma\text{-Al}_2\text{O}_3$ beads can effectively isolate $-\text{SO}_3\text{H}$ groups with H_2O molecules, hindering the progression of 5-HMF rehydration, which was also consistent with Yang's research.^[33]

$\text{Al}_2\text{O}_3-650^\circ\text{C}$, $\text{C}_3\text{-SO}_3\text{H}-\gamma\text{-Al}_2\text{O}_3-650^\circ\text{C}$, $\text{C}_8\text{-SO}_3\text{H}-\gamma\text{-Al}_2\text{O}_3-650^\circ\text{C}$ and $\text{C}_{16}\text{-SO}_3\text{H}-\gamma\text{-Al}_2\text{O}_3-650^\circ\text{C}$. In addition, the $\gamma\text{-Al}_2\text{O}_3$ beads were also used as blank experiments. The effect of the hydrophobicity of functionalized $\gamma\text{-Al}_2\text{O}_3$ beads on the dehydration of fructose to 5-HMF was shown in Figure 6. The $\gamma\text{-Al}_2\text{O}_3$ beads as catalyst had a low 5-HMF yield. But the yields of 5-HMF obtained with $\text{SO}_3\text{H}-\gamma\text{-Al}_2\text{O}_3-650^\circ\text{C}$, $\text{C}_3\text{-SO}_3\text{H}-\gamma\text{-Al}_2\text{O}_3-650^\circ\text{C}$, $\text{C}_8\text{-SO}_3\text{H}-\gamma\text{-Al}_2\text{O}_3-650^\circ\text{C}$ and $\text{C}_{16}\text{-SO}_3\text{H}-\gamma\text{-Al}_2\text{O}_3-650^\circ\text{C}$ were 52%, 66%, 70% and 84%, respectively, which indicates that the hydrophobic properties of the functionalized $\gamma\text{-Al}_2\text{O}_3$ beads could increase the yield of 5-HMF, the stronger the hydrophobicity the higher the yield of 5-HMF. This reaction further confirmed that hydrophobic groups in the $\gamma\text{-Al}_2\text{O}_3$ beads can effectively isolate $-\text{SO}_3\text{H}$ groups with H_2O molecules, hindering the progression of 5-HMF rehydration, which was also consistent with Yang's research.^[33]

2.2.2 | Effect of the calcination temperature of $\gamma\text{-Al}_2\text{O}_3$ beads on dehydration of fructose into 5-HMF

The three functionalized $\gamma\text{-Al}_2\text{O}_3$ beads with the different calcination temperatures were tested in catalytic dehydration of fructose to 5-HMF. Figure 7 shows that the 5-HMF yields obtained from fructose with $\text{C}_{16}\text{-SO}_3\text{H}-\gamma\text{-Al}_2\text{O}_3-650^\circ\text{C}$, $\text{C}_{16}\text{-SO}_3\text{H}-\gamma\text{-Al}_2\text{O}_3-850^\circ\text{C}$ and $\text{C}_{16}\text{-SO}_3\text{H}-\gamma\text{-Al}_2\text{O}_3-1000^\circ\text{C}$ were 84%, 68% and 63%, respectively, which shows that the pore structure of functionalized $\gamma\text{-Al}_2\text{O}_3$ beads has a great effect on the yields of 5-HMF. It was known from the analysis of hydrophobic properties that the decrease in the specific surface area and the active hydroxyl groups of alumina would lead to lower hydrophobicity of functionalized $\gamma\text{-Al}_2\text{O}_3$ beads. Although the average pore diameter of $\gamma\text{-Al}_2\text{O}_3$ beads increased and the diffusion resistance decreased by using high calcination temperature, the specific surface area of $\gamma\text{-Al}_2\text{O}_3$

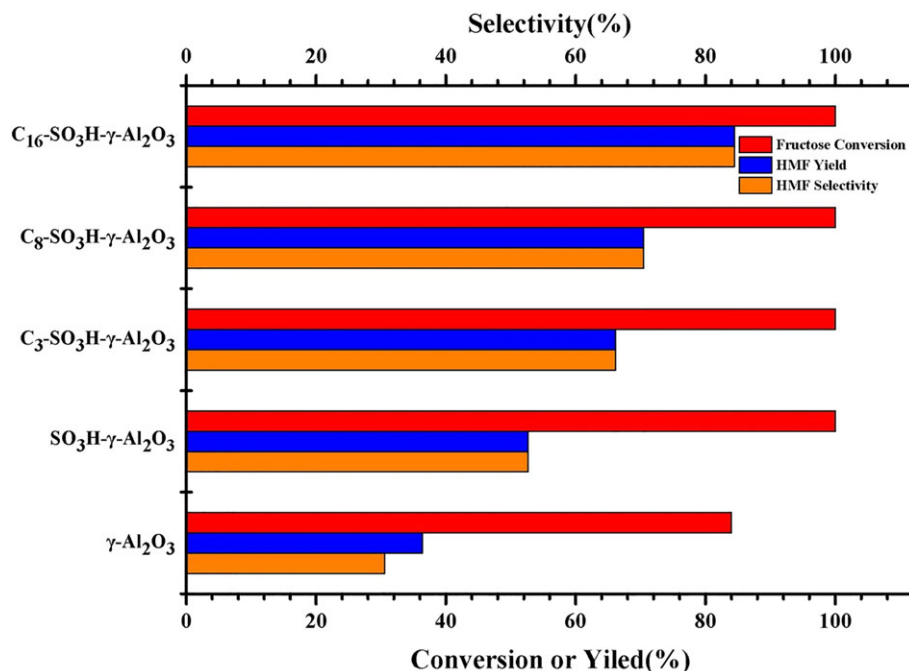


FIGURE 6 Effect of the catalyst hydrophobicity on the dehydration of fructose to 5-HMF. Reaction conditions: fructose 90 mg, SO₃H-γ-Al₂O₃-650°C 20 mg, C₃-SO₃H-γ-Al₂O₃-650°C 25 mg, C₈-SO₃H-γ-Al₂O₃-650°C 30 mg, C₁₆-SO₃H-γ-Al₂O₃-650°C 30 mg, solvents (DMSO/H₂O, V/V = 4:1), volume 1 mL, 110°C, 4 hr

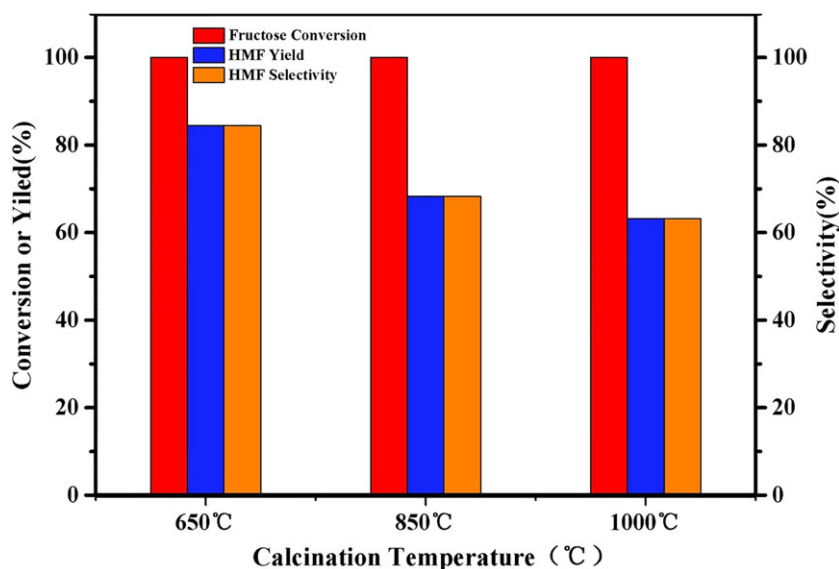


FIGURE 7 Effects of the pore structure of C₁₆-SO₃H-γ-Al₂O₃ on the dehydration of fructose to 5-HMF. Reaction conditions: fructose 90 mg, C₁₆-SO₃H-γ-Al₂O₃ beads 30 mg, solvents (DMSO/H₂O, V/V = 4:1), volume 1 mL, 110°C, 4 hr

beads and hydrophobicity of functionalized γ-Al₂O₃ beads was the key factor affecting the yield of HMF.

2.2.3 | Effect of reaction conditions on dehydration of fructose into 5-HMF

In order to be more conducive to industrial production applications, the optimal reaction conditions (i.e. reaction

medium, reaction time, temperature and catalyst amount) were investigated. Above all, the influence of reaction medium has been studied. According to previous studies,^[44,45] DMSO has been proven to be a good solvent for the production of 5-HMF and, due to economic and environmental considerations, the biphasic solvents of DMSO and H₂O with different volume ratios were considered as reaction medium in this study. At 110°C and 4 hr reaction time, the effect of reaction medium was shown

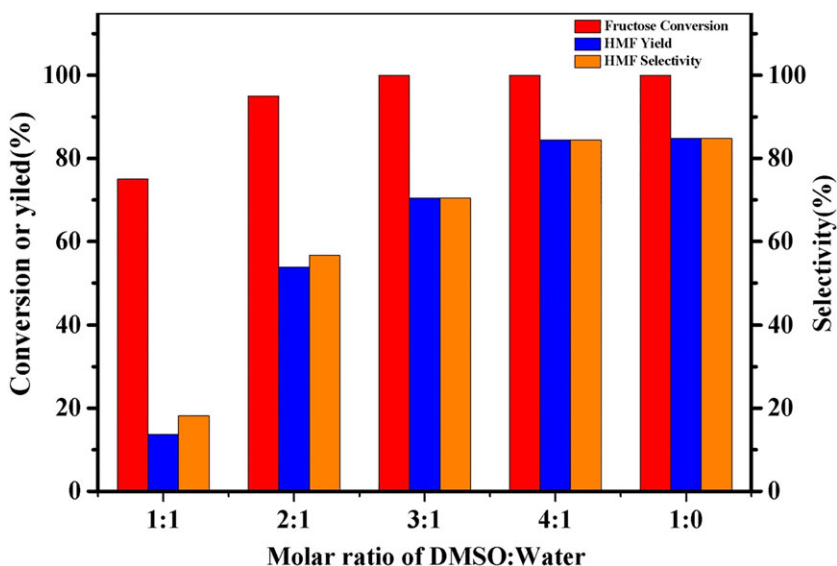


FIGURE 8 Effect of reaction medium on C_{16} -SO₃H- γ -Al₂O₃-650°C catalyzed synthesis of 5-HMF from fructose. Reaction conditions: fructose 90 mg, C_{16} -SO₃H- γ -Al₂O₃-650°C 30 mg, volume 1 mL, 110°C, 4 hr

in Figure 8. It was found that both fructose conversion and the yield of 5-HMF increased significantly with the increase of DMSO ratio in the solvent system, when DMSO/H₂O (V/V, 4:1) or pure DMSO, the yield of 5-HMF reaches a maximum of 84% with fructose conversion of 100%. It was indicated that reaction medium has an important influence on fructose conversion, especially 5-HMF yield. It was worth reminding that sulfonic acid groups play a key role in this process. According to previous literature, it was reported that the most stable form of fructose was the β -D-fructofuranoses in DMSO solution. When Bronsted acid was present in the reaction system, H⁺ prefers to interact with DMSO other than fructose, forming [DMSOH]⁺ as the catalytically active species. Catalytic fructose tautomerization to β -D-furan sugar for further dehydration produced 5-HMF.^[46] In addition, when the reaction system proceeded for more than 20

min, the color of the solution began to turn brown, gradually deepening with time, indicating the production of humins. However, when the reaction was completed, no insoluble substance was found in the catalytic system. Upon further detection by high-performance liquid chromatography (HPLC), 5-HMF was found to be the unique product with full fructose conversion, which manifested that soluble humins as byproducts were formed in this system. There was also no levulinic acid as byproduct, as was detected in previous studies.^[47] The result may be explained by the fact that DMSO can promote the dehydration of fructose to a high 5-HMF yield by maintaining the stability of 5-HMF formation. Thus, the volume ratio of DMSO/H₂O (V/V, 4:1) was chosen as reaction medium.

Catalyst amount was an important parameter for obtaining the optimal yield of products. Figure 9 shows

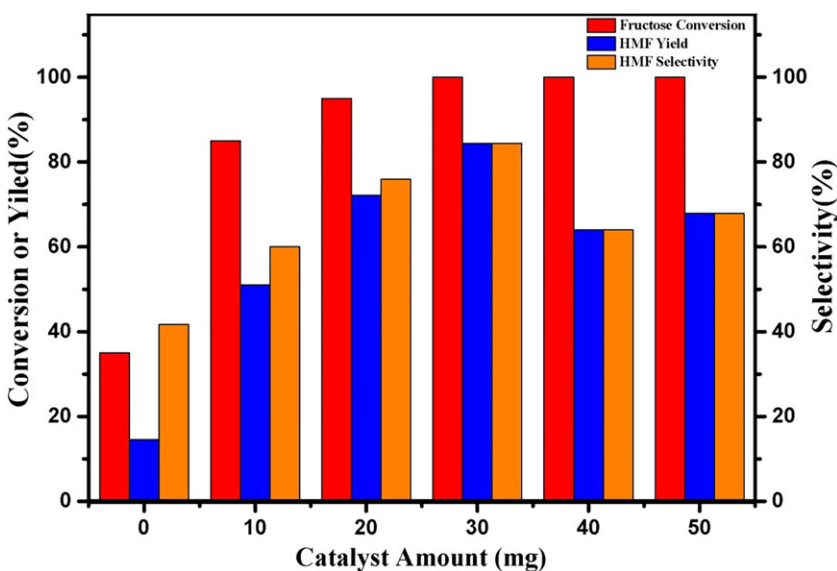


FIGURE 9 Effect of catalyst amount on C_{16} -SO₃H- γ -Al₂O₃-650°C catalyzed synthesis of 5-HMF from fructose. Reaction conditions: fructose 90 mg, solvents (DMSO/H₂O, V/V = 4:1), volume 1 mL, 110°C, 4 hr

that the results were obtained in DMSO/H₂O (V/V, 4:1) at 110°C and 4 hr. In the absence of catalyst, 14% 5-HMF yield and 35% fructose conversion were obtained, respectively. With an increase in the catalyst amount, the 5-HMF yield and selectivity and fructose conversion increased significantly, which was due to the increase in the availability of catalyst active sites. When the catalyst amount increased to 30 mg, the 5-HMF yield reached a maximum of 84% with full fructose conversion. Nevertheless, further increasing the catalyst amount decreased the 5-HMF yield to 64% (40 mg) and 67% (50 mg), which suggests that superfluous catalyst will lead to the formation of polymerization and other byproducts. With these results, we considered the catalyst amount of 30 mg as optimal for fructose dehydration to 5-HMF.

Compared with Yang's research,^[33] the optimal amount of catalyst was reduced in this catalytic system. The ratio of fructose to catalyst was 50 mg:28 mg in Yang's study, while our ratio of fructose to catalyst was 90 mg:30 mg. This was mainly related to the properties of alumina supports. On the one hand, the acid of the alumina beads was stronger than that of nano-silica, and the former had stronger catalytic capacity. A 5-HMF yield of about 10% and fructose conversion of about 20% were obtained in Yang's research with bare silica as catalyst. However, there was a 5-HMF yield of 30% and fructose conversion of 84% using the pure alumina beads as catalyst in this paper. On the other hand, the alumina catalyst had a high specific surface area and abundant porous structure, which was conducive to the loading and dispersion of active components and was beneficial to the catalytic reaction.

Reaction time and temperature played a vital role in the fructose dehydration to 5-HMF, and the results were

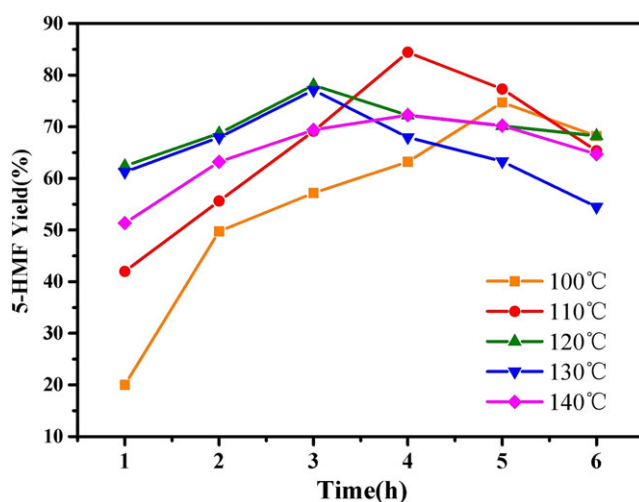


FIGURE 10 Effects of reaction temperature and time on C₁₆-SO₃H-γ-Al₂O₃-650°C catalyzed synthesis of 5-HMF from fructose. Reaction conditions: fructose 90 mg, C₁₆-SO₃H-γ-Al₂O₃-650°C 30 mg, solvents (DMSO/H₂O, V/V = 4:1), volume 1 mL

summarized in Figure 10. It was found that the yield of 5-HMF at different temperatures showed a similar trend with the extension of reaction time, which was that the 5-HMF yield increased rapidly and then decreased with time. Because the optimal reaction time was over, there would be soluble polymer and humin production in the reaction. Moreover, different reaction temperatures and reaction times correspond to different maximum 5-HMF yields. The yield of 5-HMF reached a maximum of 84% in all catalytic systems at 110°C for a reaction time of 4 hr. However, the 5-HMF yield decreased gradually when the temperature was further elevated to the higher range. It was probable that the increase in reaction temperature favors fructose dehydration, but it also increases the generation of soluble polymers and humin, thereby covering the effective active sites of the catalyst resulting in a decrease in the area of contact with the substrate. Amarasekara *et al.* also reported similar results for the decomposition of 5-HMF to unknown byproducts at high temperatures.^[48]

In summary, we obtained the highest 5-HMF yield of 84% with C₁₆-SO₃H-γ-Al₂O₃-650°C under the following reaction conditions: reaction medium of DMSO/H₂O (V/V, 4:1), catalyst amount of 30 mg, temperature of 110°C, and reaction time of 4 hr.

2.3 | The reusability and stability of the catalyst

The reusability and stability of the catalyst are important parameters to be considered when using heterogeneous catalysts in dehydration of fructose to 5-HMF in industrial applications. In Figure 11, the C₁₆-SO₃H-γ-Al₂O₃-650°C was recovered by filtering, treating with water and dried in an oven overnight at 65°C after each run, and the regeneration experiments were obtained under the optimized reaction conditions. Figure 11 showed that the reused catalyst, C₁₆-SO₃H-γ-Al₂O₃-650°C, has a slight decrease in catalytic activity, but still 79% of 5-HMF yield was maintained after five runs. This decrease was attributed to the formation of residuals such as humins or some adsorbed intermediates, which were deposited onto the catalyst surface, thereby clogging the active sites for reaction. Moreover, the color of the catalyst turns brown after five runs (Figure 6), further indicating that the humin has been chemisorbed to the catalyst surface, which will also decrease slightly the surface area and pore volume of the catalyst (Table 1). In addition, compared with the fresh C₁₆-SO₃H-γ-Al₂O₃-650°C, the reduction of acid site density, decrease of C and S elemental content of the catalyst (Table 2) as well as weakness of the FT-IR bands at

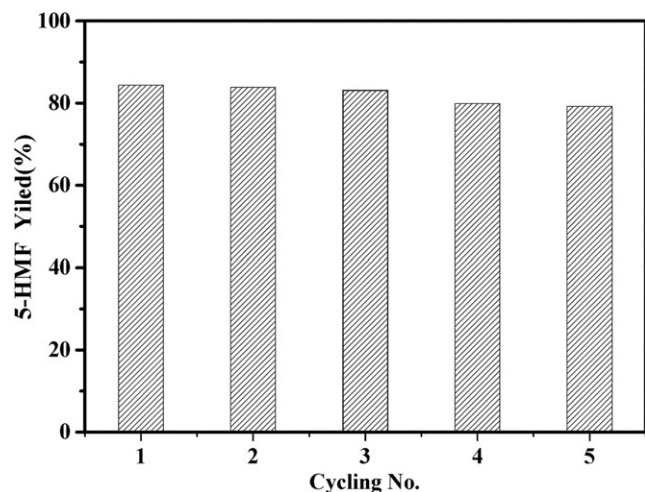


FIGURE 11 Recycling experiments of $C_{16}\text{-SO}_3\text{H-}\gamma\text{-Al}_2\text{O}_3\text{-650}^\circ\text{C}$ for the dehydration of fructose to 5-HMF. Reaction conditions: fructose 90 mg, $C_{16}\text{-SO}_3\text{H-}\gamma\text{-Al}_2\text{O}_3\text{-650}^\circ\text{C}$ 30 mg, solvents (DMSO/ H_2O , V/V = 4:1), volume 1 mL, 110°C , 4 hr

1170 cm^{-1} and 1098 cm^{-1} (Figure 4) after five repeated catalytic cycles revealed a slight loss in the active acid sites, which can lead to a decrease of catalytic performance. Although the water CA also dropped from 88.4° to 83.5° , most of the $C_{16}\text{-SO}_3\text{H-}\gamma\text{-Al}_2\text{O}_3\text{-650}^\circ\text{C}$ beads used five times can still sink in the oil phase (Figure 5), suggesting that the hydrophobicity of $C_{16}\text{-SO}_3\text{H-}\gamma\text{-Al}_2\text{O}_3\text{-650}^\circ\text{C}$ was well maintained. It was worth noting that the crush strength of $C_{16}\text{-SO}_3\text{H-}\gamma\text{-Al}_2\text{O}_3\text{-650}^\circ\text{C}$ beads after the fifth cycle was still 36.9 N per bead, which could meet the requirement of industrial applications. Therefore, the $C_{16}\text{-SO}_3\text{H-}\gamma\text{-Al}_2\text{O}_3\text{-650}^\circ\text{C}$ beads have excellent recyclability, and have great potential to be applied in industry.

3 | CONCLUSIONS

In conclusion, we successfully synthesized functionalized $\gamma\text{-Al}_2\text{O}_3$ beads with size of about 1.8 mm and crush strength over 36 N per bead. The porous structure of $\gamma\text{-Al}_2\text{O}_3$ beads facilitated the dispersion of functional groups. The loading of alkyl and sulfonic groups on the surface and internal pores of catalyst can be found by analyzing catalyst performance. Therefore, the pore structure of the supports would significantly affect the performance of the catalyst. The increase in the calcination temperature would reduce the specific surface area of supports, which cut down the hydrophobicity and activity of catalysts. Furthermore, it was shown from FT-IR and EDS analyses that competition existed between the loading of $-\text{CH}_2$ and $-\text{SH}$ groups due to the space hindrance of the long carbon chain. On one

hand, the acid site densities and hydrophobic properties of catalysts were affected by this competition. On the other hand, the effect of competition between S and C on the pore structure of catalysts also can be found by pore distribution of catalysts. The macroporous structure of the catalyst was damaged by the sulfonation process and can be protected by the alkylation process. Moreover, a less optimal amount of catalyst, a ratio of fructose to catalyst of 90 mg:30 mg, and a lower optimal reaction temperature of 110°C were presented in this paper. The highest yield of 5-HMF (84%) was obtained with the most hydrophobic catalyst $C_{16}\text{-SO}_3\text{H-}\gamma\text{-Al}_2\text{O}_3\text{-650}^\circ\text{C}$ in reaction medium DMSO/ H_2O (V/V, 4:1). Finally, the synthesized $C_{16}\text{-SO}_3\text{H-}\gamma\text{-Al}_2\text{O}_3\text{-650}^\circ\text{C}$ had certain reusability and stability for the dehydration of fructose to 5-HMF, the 5-HMF yield of $C_{16}\text{-SO}_3\text{H-}\gamma\text{-Al}_2\text{O}_3\text{-650}^\circ\text{C}$ after the fifth cycle was still 79%. There is industry potential for functional alumina as a catalyst for dehydration of fructose to 5-HMF.

4 | EXPERIMENTAL

4.1 | Materials and agents

In this work, the pseudo-boehmite (PB) powder was purchased from Tianjin Chemical Research and Design Institute. The ammonium alginate (ALG) was provided by Bright Moon Seaweed Group Company. Fructose, (3-mercaptopropyl) trimethoxysilane $[(\text{CH}_3\text{O})_3\text{Si}(\text{CH}_2)_3\text{SH}$, 95%], 5-hydroxymethylfurfural, trimethoxy (hexadecyl) silane $[(\text{CH}_3\text{O})_3\text{Si}(\text{CH}_2)_{15}\text{CH}_3$, 90%], trimethoxy (octyl) silane $[(\text{CH}_3\text{O})_3\text{Si}(\text{CH}_2)_7\text{CH}_3$, 96%] and trimethoxy (propyl)silane $[(\text{CH}_3\text{O})_3\text{Si}(\text{CH}_2)_2\text{CH}_3$, 97%] were ordered by McLean Reagent. The other agents (analytical grade) were ordered by Guangfu Fine Chemical Industry Research Institute (Tianjin, China).

4.2 | Preparation of alumina beads

Alumina beads were prepared by previous work.^[41] Then, 20 mL ALG solution (1.5 wt%) and 4 g PB powder were added into 20 mL deionized water under stirring at high speed for 15 min to form the homogeneous PB-ALG suspension, which was evenly poured into a 0.5 M $\text{Ca}(\text{NO}_3)_2$ solution. Due to the ionized gelation of ALG with metal Ca^{2+} , the semi-rigid alumina beads were formed instantly. These beads were treated with filtration, washing and acetic acid solution (0.5 M), and were finally dried at 65°C overnight and calcined at different temperature (650°C , 800°C and 1000°C) in a muffle furnace for 4 hr, and samples of $\gamma\text{-Al}_2\text{O}_3\text{-T}$ were produced (T referred to calcination temperature).

4.3 | Preparation of the functionalized alumina beads

The synthetic method of functionalized alumina beads was on the basis of previous research.^[33] A mixture of 14 mL ultrapure water, 100 mL absolute ethanol and 8.1 mL ammonium hydroxide was stirred at 40°C for 10 min. Then, the 2.24 g γ -Al₂O₃-650°C was added into the mixture. After 6 min, the prepared organosilane [i.e. (CH₃O)₃Si(CH₂)₁₅CH₃, (CH₃O)₃Si(CH₂)₇CH₃, (CH₃O)₃Si(CH₂)₂CH₃] and (CH₃O)₃Si(CH₂)₃SH were added to the mixture at intervals of 5 min. The molar ratio of [(CH₃O)₃Si(CH₂)₃SH], organosilane and alumina beads was 1:1:4. After 24 hr, the alumina beads were filtered and washed by ultrapure water, and filtered again until the solution became neutral. Then, H₂O₂ (30 wt%) solution was added to oxidize the thiol (-SH) groups to sulfonic acid groups (-SO₃X, X = NH₄⁺) at 25°C for 8 hr, followed by acidification with H₂SO₄ solution (0.8 M) at 25°C for 12 hr. The target alumina beads were obtained by filtering and washing till the solution became neutral, and were then dried at 80°C for 24 hr. Four functionalized alumina beads with sulfonic groups and different alkyls (i.e. C₀, C₃, C₈, C₁₆) were prepared, marked as SO₃H- γ -Al₂O₃-650°C, C₃-SO₃H- γ -Al₂O₃-650°C, C₈-SO₃H- γ -Al₂O₃-650°C and C₁₆-SO₃H- γ -Al₂O₃-650°C, respectively. In addition, the C₁₆-SO₃H- γ -Al₂O₃-850°C and C₁₆-SO₃H- γ -Al₂O₃-1000°C are also synthesized.

4.4 | Catalytic characterizations

Crush strength was measured by the particle strength tester. The morphology of beads and C and S contents of the alumina beads were recorded by Hitachi S-4800 scanning electron microscope at 20 kV. Grinding the functional γ -Al₂O₃ beads into powders and pressing into sheets, the water CAs of the sheet samples were analyzed on an Optical Contact Angle Measuring Device (Dataphysics, OCA15EC, Germany). Specific surface areas and pore diameters were obtained from low-temperature N₂ adsorption-desorption instrument (Quantachrome Autosorb instrument from America). The samples were outgassed for 8 hr under vacuum at 250°C prior to adsorption. The nitrogen adsorption and desorption curves were obtained at -196°C liquid nitrogen. The surface area was determined by the multipoint BET method, and the pore volume and pore size of the samples were calculated by the BJH method. FT-IR spectroscopy analysis was achieved with a spectrophotometer (BIO-Rad, Japan) with the wavenumber range of 500–4000 cm⁻¹ at a spectral resolution of 4 cm⁻¹.

4.5 | Catalytic activity test

In this process, the reactant fructose (90 mg), reaction medium (water and DMSO with different volume ratios) and catalyst (0–50 mg) were successively added to a 15-mL glass reactor with a screw top of Teflon, and stirred and heated at a certain stated temperature. Timing was started when the oil bath temperature reached the set temperature. After the reaction was completed, the reactor was cooled down to room temperature in flowing cold water, and then the sample was diluted to 50 mL with ultrapure water. Then, 1 mL of the solution was taken out with a syringe, filtered through a 0.22- μ m syringe filter, and the resulting sample was subjected to HPLC analysis using a refractive index detector. Using 0.004 M H₂SO₄ solution as the mobile phase, samples were separated using an Aminex HPX-87H 300 mm \times 7.8 mm column, and the column temperature was designed at 65°C. Identification of the compounds was calibrated with a reference sample. Fructose conversion, 5-HMF yield and selectivity were carbon base evaluated as follows:

Fructose conversion (mol%) = (1 – fructose concentration in product/fructose concentration in the sample);

5-HMF yield (mol%) = moles of carbon in 5-HMF/ moles of carbon loaded in fructose \times 100%;

5-HMF selectivity (mol%) = 5-HMF yield/fructose conversion \times 100%.

ACKNOWLEDGEMENTS

The authors thank the National Key R&D Program of China (No. 2017YFB0306502) and the Natural Science Foundation of Tianjin, China (No. 16JCYBJC19600) for financial support.

ORCID

Fang Lin  <https://orcid.org/0000-0002-7929-0527>

Kang Wang  <https://orcid.org/0000-0002-1451-2360>

REFERENCES

- [1] X. Liu, J. Xiao, H. Ding, W. Zhong, Q. Xu, S. Su, D. Yin, *Chem. Eng. J.* **2016**, 283, 1315.
- [2] I. Sádaba, Y. Y. Gorbanev, S. Kegnaes, S. S. R. Putluru, R. W. Berg, A. Riisager, *ChemCatChem* **2013**, 5, 284.
- [3] N. K. Gupta, S. Nishimura, A. Takagaki, K. Ebitani, *Green Chem.* **2011**, 13, 824.
- [4] L. Gao, K. Deng, J. Zheng, B. Liu, Z. Zhang, *Chem. Eng. J.* **2015**, 270, 444.
- [5] G. W. Huber, J. N. Chheda, C. J. Barrett, J. A. Dumesic, *Science* **2005**, 308, 1446.

- [6] S. Yao, X. Wang, Y. Jiang, F. Wu, X. Chen, X. Mu, *ACS Sustainable Chem. Eng.* **2014**, 2, 173.
- [7] J. Zhang, E. Weitz, *ACS Catal.* **2012**, 2, 1211.
- [8] Y. Yang, C. W. Hu, M. M. Abu-Omar, *Mol. Catal. A Chem.* **2013**, 376, 98.
- [9] N. Jiang, R. Huang, W. Qi, R. X. Su, Z. M. He, *Bio Energy Res.* **2012**, 5, 380.
- [10] H. Zhao, J. E. Holladay, H. Brown, Z. C. Zhang, *Science* **2007**, 316, 1597.
- [11] Z. Cao, M. Li, Y. Chen, T. Shen, C. L. Tang, C. J. Zhu, H. J. Ying, *Appl. Catal. A* **2019**, 569, 93.
- [12] A. H. Jadhav, H. Kim, I. T. Hwang, *Bioresour. Technol.* **2013**, 132, 342.
- [13] Y. Qu, C. Huang, J. Zhang, B. Chen, *Bioresour. Technol.* **2012**, 106, 170.
- [14] P. Khemthong, P. Daorattanachai, N. Laosiripojana, K. Faungnawakij, *Cat. Com.* **2012**, 29, 96.
- [15] X. H. Qi, M. Watanabe, T. M. Aida, R. L. Smith Jr., *Green Chem.* **2008**, 10, 799.
- [16] X. H. Qi, M. Watanabe, T. M. Aida, R. L. Smith Jr., *Ind. Eng. Chem. Res.* **2008**, 47, 9234.
- [17] X. H. Qi, M. Watanabe, T. M. Aida, R. L. Smith Jr., *Cat. Com.* **2009**, 10, 1771.
- [18] J. Chen, K. Li, L. Chen, R. Liu, X. Huang, D. Ye, *Green Chem.* **2014**, 16, 2490.
- [19] C. Tian, C. Bao, A. Binder, Z. Zhu, B. Hu, Y. Guo, B. Zhao, S. Dai, *Chem. Commun.* **2013**, 49, 8668.
- [20] X. Guo, Q. Cao, Y. Jiang, J. Guan, X. Wang, X. Mu, *Carbohydr. Res.* **2012**, 351, 35.
- [21] X. Qi, H. Guo, L. Li, R. L. Smith, *ChemSusChem* **2012**, 5, 2215.
- [22] H. Wang, Q. Kong, Y. Wang, T. Deng, C. Chen, X. Hou, Y. Zhu, *ChemCatChem* **2014**, 6, 728.
- [23] L. Hu, X. Tang, Z. Wu, L. Lin, J. X. Xu, N. Xu, B. L. Dai, *Chem. Eng. J.* **2015**, 263, 299.
- [24] Y. Q. Wang, G. Q. Ding, X. H. Yang, H. Y. Zheng, Y. L. Zhu, Y. W. Li, *Appl. Catal. B* **2018**, 235, 150.
- [25] Y. Li, H. Liu, C. Song, X. Gu, H. Li, W. Zhu, S. Yin, C. Han, *Bioresour. Technol.* **2013**, 133, 347.
- [26] D. A. Kotadia, S. S. Soni, *Cat. Sci. Technol.* **2013**, 3, 469.
- [27] X. Tong, Y. Li, *ChemSusChem* **2010**, 3, 350.
- [28] C. Lansalot-Matras, C. Moreau, *Cat. Com.* **2003**, 4, 517.
- [29] Y. Román-Leshkov, J. N. Chheda, J. A. Dumesic, *Science* **2006**, 312, 1933.
- [30] Y. Román-Leshkov, J. A. Dumesic, *Top. Catal.* **2009**, 52, 297.
- [31] G. Q. Lv, L. L. Deng, B. Q. Lu, J. L. Li, X. L. Hou, Y. X. Yang, *J. Clean. Prod.* **2017**, 142, 2244.
- [32] L. Wang, H. Wang, F. Liu, A. Zheng, J. Zhang, Q. Sun, J. P. Lewis, L. Zhu, X. Meng, F. S. Xiao, *ChemSusChem* **2014**, 7, 402.
- [33] Z. Yang, W. Qi, R. Huang, J. Fang, R. Su, Z. He, *Chem. Eng. J.* **2016**, 296, 209.
- [34] Y. Yao, Z. Gu, Y. Wang, H. J. Wang, W. Li, *Russ. J. Gen. Chem.* **2016**, 86, 1698.
- [35] J. S. Valente, S. Falcón, E. Lima, M. A. Vera, P. Bosch, E. López Salinas, *Micropor. Mesopor. Mater.* **2006**, 94, 277.
- [36] J. S. Valente, E. López Salinas, X. Bokhimi, J. Flores, A. M. Maubert, E. Lima, *Phys. Chem. C* **2009**, 113, 16 476.
- [37] V. Smuleac, D. A. Butterfield, S. K. Sikdar, R. S. Varma, D. Bhattacharyya, *Membr. Sci.* **2005**, 251, 169.
- [38] C. S. Maldonado, J. R. De la Rosa, C. J. Lucio-Ortiz, J. S. Valente, M. J. Castaldi, *Fuel* **2017**, 198, 134.
- [39] F. J. Morales-Leal, J. R. Rosa, C. J. Lucio-Ortiz, D. A. De Haro-Del Rio, C. S. Maldonado, S. Wi, L. B. Casabianca, C. D. Garcia, *Appl. Catal. B* **2019**, 244, 250.
- [40] K. Wang, G. Y. Meng, W. J. Yang, H. B. Yu, Y. M. Sun, X. Y. Li, *Tianjin Univ. (Sci. Technol.)* **2014**, 47, 1052. (in Chinese)
- [41] A. H. Dong, K. Wang, S. Z. Zhu, G. B. Yang, X. T. Wang, *Fuel Process. Technol.* **2017**, 158, 218.
- [42] D. Yang, B. Paul, W. Xu, Y. Yuan, E. Liu, X. Ke, *Water Res.* **2010**, 44, 741.
- [43] R. J. Kalbasi, A. R. Massah, B. Daneshvarnejad, *Appl. Clay Sci.* **2012**, 55, 1.
- [44] J. Zhang, A. Das, R. S. Assary, L. A. Curtiss, E. Weitz, *Appl. Catal. B* **2016**, 181, 874.
- [45] J. Wang, W. Xu, J. Ren, X. Liu, G. Lu, Y. Wang, *Green Chem.* **2011**, 13, 2678.
- [46] L. K. Ren, L. F. Zhu, T. Qi, J. Q. Tang, H. Q. Yang, C. W. Hu, *ACS Catal.* **2017**, 7, 2199.
- [47] Y. Shen, J. K. Sun, Y. X. Yi, B. Wang, F. Xu, R. C. Sun, *J. Mol. Catal. A Chem.* **2014**, 394, 114.
- [48] A. S. Amarasekara, L. D. Williams, C. C. Ebede, *Carbohydr. Res.* **2008**, 343, 3021.

SUPPORTING INFORMATION

Additional supporting information may be found online in the Supporting Information section at the end of the article.

How to cite this article: Lin F, Wang K, Gao L, Guo X. Efficient conversion of fructose to 5-hydroxymethylfurfural by functionalized γ -Al₂O₃ beads. *Appl Organometal Chem.* 2019;33:e4821. <https://doi.org/10.1002/aoc.4821>